



Unipolar nonvolatile memory devices with composites of poly(9-vinylcarbazole) and titanium dioxide nanoparticles

Byungjin Cho, Tae-Wook Kim, Minhyeok Choe, Gunuk Wang, Sunghoon Song, Takhee Lee *

Department of Materials Science and Engineering, Gwangju Institute of Science and Technology, Gwangju 500-712, Republic of Korea

ARTICLE INFO

Article history:

Received 11 November 2008

Received in revised form 31 January 2009

Accepted 1 February 2009

Available online 8 February 2009

PACS:

73.61.Ph

84.37.+q

85.35.-p

Keywords:

Nonvolatile unipolar memory

Filamentary conduction

Poly(9-vinylcarbazole)

Titanium dioxide nanoparticles

ABSTRACT

Organic-based devices with an 8×8 array structure using titanium dioxide nanoparticles (TiO_2 NPs) embedded in poly(9-vinylcarbazole) (PVK) film exhibited bistable resistance states and a unipolar nonvolatile memory effect. TiO_2 NPs were a key factor for realizing the bistability and the concentration of TiO_2 NPs influenced ON/OFF ratio. From electrical measurements, switching mechanism of PVK: TiO_2 NPs devices was closely associated with filamentary conduction model and it was found that the OFF state was dominated by thermally activated transport while the ON state followed tunneling transport. PVK: TiO_2 NPs memory devices in 8×8 array structure showed a uniform cell-to-cell switching, stable switching endurance, and a high retention time longer than 10^4 s.

Crown Copyright © 2009 Published by Elsevier B.V. All rights reserved.

1. Introduction

Several types of organic electronics, including organic light emitting diodes, transistors, solar cells, and nonvolatile memory devices, have attracted considerable attention due to a variety of advantages such as printability, flexibility, low processing cost, and easy fabrication [1–4]. Among these organic electronics, organic memory devices have been investigated as a promising alternative to the conventional semiconductor-based nonvolatile memory devices [5–10]. In particular, organic memory devices employing nanoparticles in the active memory materials have been extensively studied due to easily controllable processing factors such as different kinds of particles, particle size, and concentration of particles [11–13]. Much research has been done to construct organic memory devices with

high specifications including highly reproducible electrical characteristics, a large ON/OFF ratio, and a long retention time by optimizing these processing factors [11–14]. Bozano et al. showed that different types of nanoparticles (NPs) in hybrid organic–inorganic switching devices could tune the memory performance parameters such as threshold voltages and the ON/OFF ratio [14]. As compared with the organic memory devices with metallic NPs, relatively few studies have been conducted on the organic memory devices containing semiconducting NPs [15,16]. Memory devices with the hybrid organic–semiconducting NPs composites have been particularly attractive due to their unique advantages of low cost, inert chemical properties, and feasibility of various chemical compositions [15,16]. Li et al. reported data for bistability and operating mechanisms of memory devices fabricated with core/shell-type CdSe/ZnS NPs and chemically self-assembled ZnO NPs [15,16]. However, the detailed memory performances such as cell-to-cell uniformity, distribution of threshold voltages, and endurance cycles, which must be considered

* Corresponding author. Tel.: +82 62 9702313; fax: +82 62 9702304.

E-mail address: tleee@gist.ac.kr (T. Lee).

for realistic memory device application, have not been thoroughly investigated.

In this study, we report on the operation and performance of unipolar resistive switching devices involving titanium dioxide nanoparticles (TiO_2 NPs) embedded in a poly(9-vinylcarbazole) (PVK) matrix layer in an 8×8 cross-bar array structure. The switching mechanism and the charge transport were studied by electrical measurements. The statistical distribution of the ON and OFF states in the 8×8 cell array was investigated to quantify cell-to-cell uniformity. Endurance cycle and retention tests were also performed to evaluate the performance of the memory devices.

2. Experimental

Organic memory devices using TiO_2 NPs embedded in poly(9-vinylcarbazole) (PVK) in the 8×8 cross-bar array structure were fabricated on indium tin oxide (ITO) (sheet resistance of $\sim 8 \Omega/\square$) on glass substrates. ITO-coated glass substrates were pre-cleaned with a typical ultrasonic cleaning process. ITO electrodes with 8 line patterns of $100 \mu\text{m}$ line-width were prepared as bottom electrodes (Fig. 1) by conventional photolithography and a subsequent etching process. PVK (molecular weight $\sim 1,100,000$) and TiO_2 NPs (anatase 5 nm) were used to make a mixture (PVK: $\text{TiO}_2 = 200:1, 150:1, 100:1, 10:1$, and $1:1$ solution volume ratios) of PVK solution (5 mg/ml) and TiO_2 NPs solution (2 mg/ml) dissolved in 1,2-dichloroethane. The PVK: TiO_2 NPs solution was spin-coated at 4000 rpm for 40 s in a N_2 -filled glove box and the thickness of the resulting film was measured to be ~ 60 nm (for the case of PVK: $\text{TiO}_2 = 150:1$ volume ratio). To improve film

uniformity and remove residual solvent from the film, a baking process was performed on a hotplate in the N_2 -filled glove box at 150°C for 2 min. Then, Al (100 nm thick) electrodes were deposited using an e-beam evaporator at a pressure of $\sim 10^{-7}$ torr. Fig. 1a shows a schematic of the ITO/PVK: TiO_2 NPs/Al memory devices in the 8×8 cross-bar array structure. An optical image of the fabricated memory devices is displayed in Fig. 1b. Fig. 1c shows a schematic cross-sectional view, illustrating the PVK: TiO_2 NPs composite layer sandwiched between ITO and Al. Aggregates of TiO_2 NPs, having a diameter of 20–40 nm, were found within PVK matrix and the size of individual TiO_2 NP was found as 3 to 7 nm as shown in the inset of Fig. 1d. As the PVK: TiO_2 NPs volume ratio changed from 200:1 to 1:1 (i.e., the TiO_2 NPs concentration was increased), stronger aggregation of NPs was observed.

3. Results and discussion

3.1. Switching characteristics

Fig. 2a shows current–voltage (I – V) characteristics of a memory cell in the 8×8 cross-bar array devices consisting of the ITO/PVK: TiO_2 NPs (volume ratio 150:1)/Al structure. As the voltage was swept to a positive bias, the memory device exhibited an abrupt increase of current by three orders of magnitude near 3.4 V (set voltage), indicating an electrical resistance transition from a high resistance state (OFF state) to a low resistance state (ON state) (1st sweep). When the applied bias was higher than the set voltage, the device still remained in the ON state until 5.7 V (reset voltage). Beyond the reset voltage, a sharp decrease in the current occurred, showing a negative differential resistance

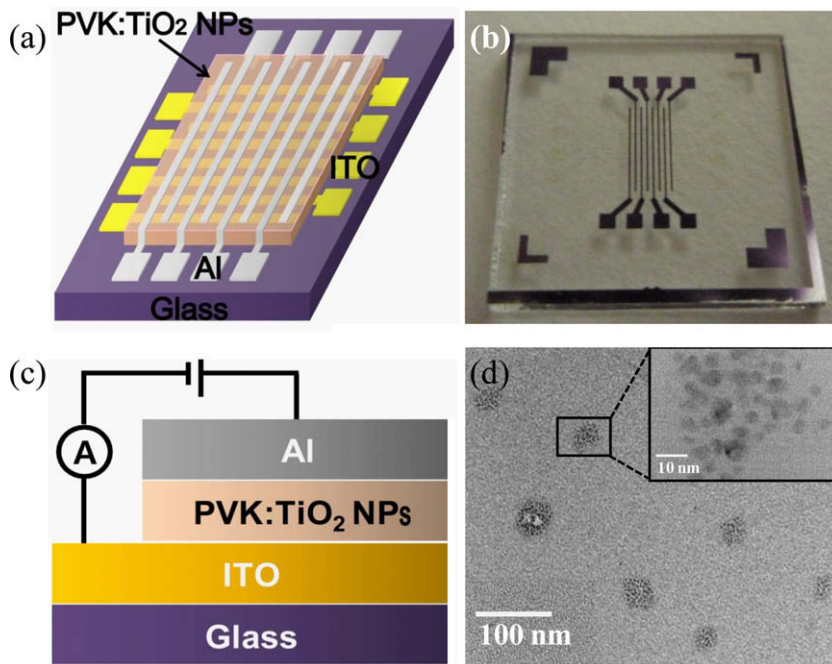


Fig. 1. (a) Schematic and (b) optical image of ITO/PVK: TiO_2 NPs/Al memory devices in an 8×8 array structure. (c) Schematic of the cross-sectional view of ITO/PVK: TiO_2 NPs/Al structure. (d) TEM image of a composite film with PVK: TiO_2 NPs volume ratio of 150:1.

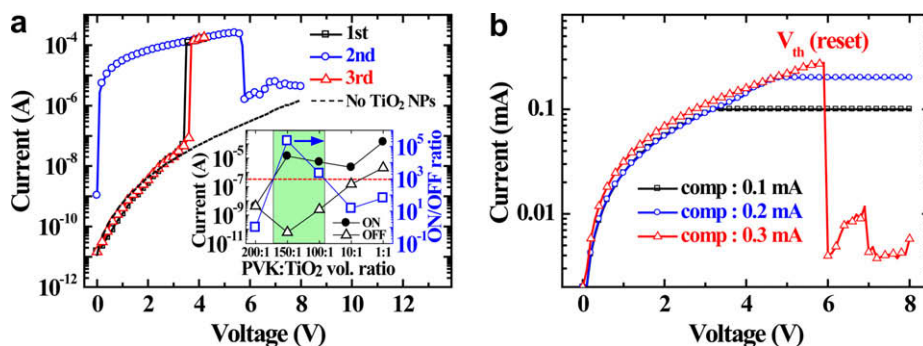


Fig. 2. (a) I - V characteristics of a ITO/PVK:TiO₂ NPs (volume ratio of 150:1)/Al memory device (line + symbol curves) and ITO/PVK/Al device without TiO₂ NPs (dashed line). The inset shows ON and OFF currents (left axis) and ON/OFF ratio (right axis) measured at 0.5 V as a function of PVK:TiO₂ NPs volume ratio. (b) Turn-off process as a function of compliance current.

(NDR) behavior (2nd sweep). The NDR phenomenon has been reported elsewhere in other polymer-based memory devices [11,17]. The current beyond the NDR region (>5.7 V) appeared to continue on a trend extending from OFF state. When the I - V characteristics were measured again (3rd sweep), the device exhibited an almost equivalent track of the current that was shown during the 1st sweep, indicating a rewritable memory effect. Therefore, the device could be set from OFF to ON (writing) by applying a voltage slightly higher than the set voltage and reset from ON to OFF (erasing) by a voltage beyond the NDR region. In this system, the switching can be achieved by successive application of voltages of the same polarity, which is typical unipolar memory effect. From the I - V characteristics described above, two different resistances at the same voltage could be obtained below the set voltage and remained stable even after the power was turned off, indicating the nonvolatile memory effect. However, devices made with just PVK without TiO₂ NPs showed no resistive switching behavior (dashed line in Fig. 2a). These effects clearly demonstrate that TiO₂ NPs play an important role in the electrical bistability phenomenon.

To investigate the role of TiO₂ NPs in the bistable switching, we performed I - V measurements on devices with different TiO₂ NPs concentration. The ON and OFF state currents measured at 0.5 V are plotted as a function of PVK:TiO₂ NPs volume ratio, as shown in the inset of Fig. 2a (left axis). It can be seen clearly that the OFF current gradually increased with increasing TiO₂ NPs concentration while the ON current remained nearly constant regardless of TiO₂ NPs concentration. These different concentration-dependent features between ON and OFF currents eventually resulted in the large variation in the ON/OFF ratios, as summarized in the inset of Fig. 2a (right axis). Especially, NPs concentrations in the range from $\sim 150:1$ to $100:1$ volume ratio was observed to realize organic memory devices with high ON/OFF ratio more than three orders of magnitude. Therefore, the TiO₂ NPs concentration can be a critical factor for determining ON/OFF ratio, one of the key parameters of the memory operation. Contrary to OFF currents, ON currents show relatively little variation regardless of TiO₂ NPs concentration. It reveals that high current states are attributed to the introduction of TiO₂ NPs.

Specifically, the conduction process of ON state is consistent with the filamentary conduction model [18]. The model invokes the formation of filaments in the PVK polymer, exhibiting ohmic conduction without thermal activation. The fracture of the filaments is probably a consequence of Joule heating, raising the temperature of a part of the filament. The Joule heating effect gives rise to atomic reorganization. In our device, the filamentary paths are not only made by defects or structural disorder within the PVK polymer. TiO₂ NPs also become involved in formation of the filamentary paths. Growth of the filamentary paths may occur mainly in the localized region where TiO₂ NPs are distributed. TiO₂ NPs serve as one element source of materials which constitute the high conducting paths. It is reasonable to assume that the filament consists of TiO₂ NPs and some kind of defect within the PVK. Note that others have reported the bistability switching in PVK materials [19]. However the electrode materials, device structures, PVK layer thickness, and charge conduction behavior are different from our devices [20], which may explain different switching properties.

PVK is well known as a hole transporting material [21]. Some reports on polymer memory devices using PVK or PVK composite with NPs suggested that holes can serve as major carriers to cause the memory effect [19,22]. Furthermore, hole injection barrier of PVK is much lower than electron injection barrier because of the relatively high highest occupied molecular orbital (HOMO) energy level of PVK. Thus, holes will be the major charge carriers responsible for the memory effect. PVK mainly functions as matrix where filamentary paths are formed.

Fig. 2b shows the turn-off process as a function of compliance current. Once the ON state was formed, the OFF state could be obtained only when enough compliance current was applied to the devices. The turn-off process of the memory devices could be triggered only by the appropriate compliance current. In Fig. 2b, the device did not turn to the OFF state if the compliance current was set at 1 mA or 2 mA, but it successfully turned to the OFF state when the compliance current was set larger than 3 mA. A similar compliance dependency of the turn-off process has been reported for the case of memory devices with the Al/PVK/Al structure previously [19]. Our device showed considerable noise fluctuations beyond the NDR region. The noise

might have been closely related with rupturing and regrowing of conducting filaments inside the PVK polymer on the filament model [18]. The number of mobile carriers and their mobility would have provoked noise fluctuations. The considerable noise fluctuations generally occurred within the NDR region which displayed a gradual decrease of current [18,23], whereas the noise of our devices appeared after the NDR region (Fig. 2b). Note that some reports suggested that the bistability of the organic nonvolatile memory devices is attributed to the effect of an interfacial oxide layer such as Al_2O_3 [24,25]. In order to minimize the possible effect of the thin native oxide, the Al top electrode was deposited on the composite film with a delay time as small as possible. In addition, to minimize O_2 and H_2O effects, all electrical measurements were performed in a nitrogen filled glove box.

To obtain further information about the switching characteristics of the devices, we examined the correlation between the set current (current at the set voltage) and the reset current (current at the reset voltage). As shown in Fig. 3, we found that the reset current gradually increased as increasing the set current. This correlation between reset and set currents can also be used to understand the mechanism of memory operation associated with the filamentary conduction model [19,26]. It is expected that the higher set current will form stronger filaments. On the other hand, if the stronger filaments are formed, it is hard to break the filamentary current path, and thus the higher reset current should be expected.

3.2. Charge transport mechanism

The charge transport mechanism was studied by temperature-variable I - V measurements in a vacuum pressure of $\sim 10^{-3}$ torr. Fig. 4 is the Arrhenius plot of the ON and OFF state currents in the temperature range from 150 to 300 K. The ON and OFF currents were read at 2 V while the temperature was swept at a speed of 2 K/min. The OFF current can be explained by a thermally activated transport with an activation energy of ~ 66 meV. In contrast, the ON current was almost temperature-independent, exhibiting negligible activation energy of ~ 3 meV. It was found that the log-log plot of the ON current clearly exhibited the form of I - V , indicating ohmic characteristics (Fig. 4 inset). These features of the ON current are mainly attributed to charge

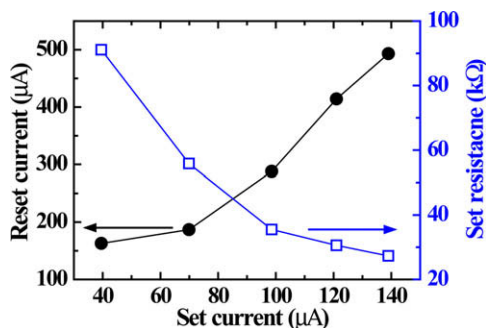


Fig. 3. Reset current (left axis) and set resistance (right axis) as a function of set current for a ITO/PVK: TiO_2 NPs (volume ratio of 150:1)/Al memory device.

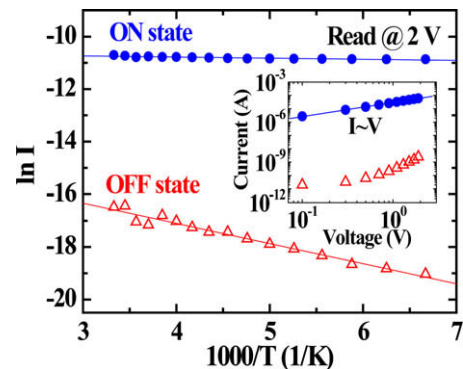


Fig. 4. Arrhenius plot of ON and OFF currents at temperature range from 150 to 300 K for a ITO/PVK: TiO_2 NPs (volume ratio of 150:1)/Al device. The inset shows the log-log plot of I - V characteristics in the voltage range of 0 to 2 V at 300 K.

tunneling through filamentary paths induced by high electric field [18,24,27]. Consequently, bistable resistance switching of PVK: TiO_2 NPs devices accompanies the change of charge conduction mechanism from thermally activated transport (OFF state) into tunneling transport (ON state).

3.3. Memory performance

For practical memory device applications, the cell-to-cell uniformity of memory array devices is critical. Fig. 5 shows the cumulative probability data of ITO/PVK: TiO_2 NPs/Al memory devices, exhibiting a good cell-to-cell uniformity. Our memory devices have a narrow distribution in both the ON and OFF states. Particularly, the OFF state showed less variable resistance due to the insulating property of the PVK polymer. The statistical distribution of both the set and reset threshold voltages was obtained from repetitive sweeping operation of a single cell, as shown in the inset of Fig. 5. Both distributions of the set and reset threshold voltages were fitted with Gaussian functions with 3σ (three standard deviations), shown as black curves in the inset. The set voltages were mainly distributed from 2.5 to 4 V, and the reset voltages ranged widely from 5 to

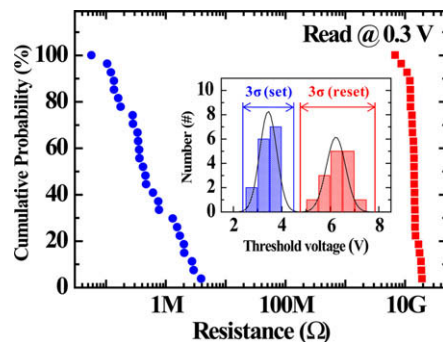


Fig. 5. A cumulative probability data set of ITO/PVK: TiO_2 NPs (volume ratio of 150:1)/Al memory devices, exhibiting a good cell-to-cell uniformity. The inset shows the distribution of set and reset threshold voltages from repetitive sweep cycles from a single working cell. Both distributions were fitted with Gaussian functions with 3σ (three standard deviations), shown as black curves in the inset.

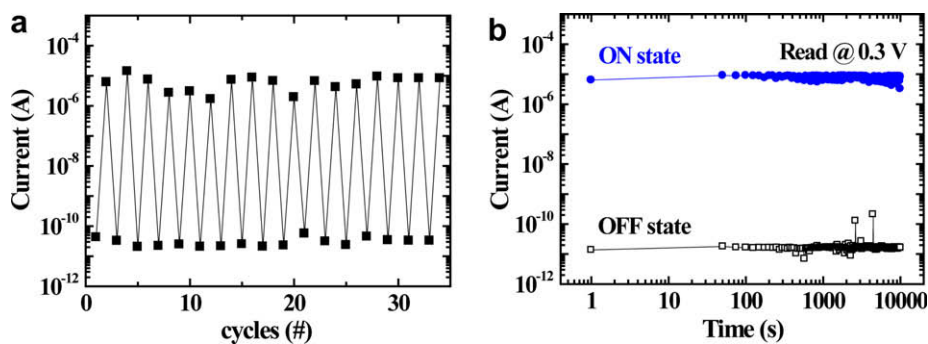


Fig. 6. (a) Endurance cycles obtained by repetitive sweeping and (b) retention time characteristics of the two resistance states under 0.3 V constant voltage stress.

7.5 V, showing a difference of ~ 1 V. Thus, the distribution of each threshold voltage was fairly separated enough to be utilized for potential memory application. The substantial distribution of switching voltages is especially important for determining the operative voltages of resistance-based memory devices which can be definitely distinguished between the OFF and ON state.

The performance evaluation of the memory devices was checked by endurance and retention tests. Fig. 6a shows the sweep endurance of the PVK:TiO₂ NPs memory devices. The initial state for the device was OFF, and, after sweeping by 4.3 V, the ON state was achieved. The state of the devices (ON or OFF) could be determined by measuring the current at a read voltage of 0.3 V. Two stable resistance states with a high ON/OFF ratio were achieved, which can provide improved information storage ability by precise control over the ON and OFF states. In addition, the retention test result is shown in Fig. 6b. The PVK:TiO₂ NPs memory devices presented reasonably good retention characteristics for 10^4 s without significant current degradation, maintaining an ON/OFF ratio of over 10^5 . However, the formed filamentary paths will become gradually weak. It indicates that the device cannot keep the ON state any more after a long time.

4. Conclusions

In summary, we demonstrated unipolar nonvolatile resistive switching devices with an 8×8 array structure based on composites of PVK and TiO₂ NPs. The TiO₂ NP induced the bistability and its concentration within PVK was a critical factor to control ON/OFF ratio. From electrical characterizations, the switching was mainly governed by the filamentary conduction mechanism and the transport accompanied the change from thermally activated transport (OFF state) into tunneling transport (ON state). The PVK:TiO₂ NPs memory devices showed uniform cell-to-cell switching, stable endurance, and good retention, which feature a potential application for nonvolatile memory devices.

Acknowledgements

This work was supported by the National Research Laboratory (NRL) Program of the Korea Science and Engineer-

ing Foundation (KOSEF), the Program for Integrated Molecular System at GIST, and System IC 2010 project of Korea Ministry of Knowledge Economy.

References

- [1] S.H. Park, Y. Jin, J.Y. Kim, S.H. Kim, J. Kim, H. Suh, K. Lee, *Adv. Funct. Mater.* 17 (2007) 3063.
- [2] Y. Chen, G.-Y. Jung, D.A.A. Ohlberg, X. Li, D.R. Stewart, J.O. Jeppesen, K.A. Nielsen, J.F. Stoddart, R.S. Williams, *Nanotechnology* 14 (2003) 462.
- [3] J.Y. Kim, K. Lee, N.E. Coates, D. Moses, T.-Q. Nguyen, M. Dante, A.J. Heeger, *Science* 317 (2007) 222.
- [4] J. Ouyang, C.-W. Chu, C.R. Szmanda, L. Ma, Y. Yang, *Nat. Mater.* 3 (2004) 918.
- [5] K. Galatsis, K. Wang, Y. Botros, Y. Yang, Y.-H. Xie, J.F. Stoddart, R.B. Kaner, C. Ozkan, J. Liu, M. Ozkan, C. Zhou, K.W. Kim, *IEEE Circ. Dev. Mag.* 22 (2006) 12.
- [6] J.C. Scott, L.D. Bozano, *Adv. Mater.* 19 (2007) 1452.
- [7] E.Y.H. Teo, Q.D. Ling, Y. Song, Y.P. Tan, W. Wang, E.T. Kang, D.S.H. Chan, C. Zhu, *Org. Electron.* 7 (2006) 173.
- [8] J. Chen, D. Ma, *J. Appl. Phys.* 100 (2006) 034512.
- [9] F. Verbakel, S.C.J. Meskers, R.A.J. Janssen, H.L. Gomes, A.J.M. van den Biggelaar, D.M. de Leeuw, *Org. Electron.* 9 (2008) 829.
- [10] B.C. Das, A.J. Pal, *Org. Electron.* 9 (2008) 39.
- [11] R.J. Tseng, J. Huang, J. Ouyang, R.B. Kaner, Y. Yang, *Nano Lett.* 5 (2005) 1077.
- [12] D.T. Simon, M.S. Griffo, R.A. DiPietro, S.A. Swanson, S.A. Carter, *Appl. Phys. Lett.* 89 (2006) 133510.
- [13] Y. Song, Q.D. Ling, S.L. Lim, E.Y.H. Teo, Y.P. Tan, L. Li, E.T. Kang, D.S.H. Chan, C. Zhu, *IEEE Electron. Dev. Lett.* 28 (2007) 107.
- [14] L.D. Bozano, B.W. Kean, M. Beinhoff, K.R. Carter, P.M. Rice, J.C. Scott, *Adv. Funct. Mater.* 15 (2005) 1933.
- [15] F. Li, T.W. Kim, W. Dong, Y.H. Kim, *Appl. Phys. Lett.* 92 (2008) 011906.
- [16] F. Li, D.I. Son, S.M. Seo, H.M. Cha, H.J. Kim, B.J. Kim, J.H. Jung, T.W. Kim, *Appl. Phys. Lett.* 91 (2007) 122111.
- [17] L.D. Bozano, B.W. Kean, V.R. Deline, J.R. Salem, J.C. Scott, *Appl. Phys. Lett.* 84 (2004) 607.
- [18] G. Dearnaley, A.M. Stoneham, D.V. Morgan, *Rep. Prog. Phys.* 33 (1970) 1129.
- [19] Y.-S. Lai, C.-H. Tu, D.-L. Kwong, J.S. Chen, *Appl. Phys. Lett.* 87 (2005) 122101.
- [20] Y.-S. Lai, C.-H. Tu, D.-L. Kwong, J.S. Chen, *IEEE Electron. Dev. Lett.* 27 (2006) 451.
- [21] Q.D. Ling, S.L. Lim, Y. Song, C.X. Zhu, D.S.H. Chan, E.T. Kang, K.G. Neoh, *Langmuir* 23 (2007) 312.
- [22] D.-I. Son, J.-H. Kim, D.-H. Park, W.K. Choi, F. Li, J.H. Ham, T.W. Kim, *Nanotechnology* 19 (2008) 055204.
- [23] G. Dearnaley, D.V. Morgan, A.M. Stoneham, *J. Non-Cryst. Solids* 4 (1970) 593.
- [24] M. Cölle, M. Büchel, D.M. de Leeuw, *Org. Electron.* 7 (2006) 305.
- [25] F. Verbakel, S.C.J. Meskers, R.A.J. Janssen, *Appl. Phys. Lett.* 91 (2007) 192103.
- [26] W. Guan, S. Long, Q. Liu, M. Liu, W. Wang, *IEEE Electron. Dev. Lett.* 29 (2008) 434.
- [27] H.S. Majumdar, J.K. Baral, A. Laiho, J. Ruokolainen, O. Ikkala, R. Österbacka, *Adv. Mater.* 18 (2006) 2805.